European Review for Medical and Pharmacological Sciences 2020; 24: 9438-9452

Long noncoding RNA Linc00210 promotes non-small cell lung cancer progression *via* sponging miR-16-5p/PTK2 axis

Q. PENG[1], Y. CHEN[1], C.-N. LI[2]

[1]Department of Respiration, Shangluo Central Hospital, Shangluo, Shanxi, China
[2]Department of Internal Medicine, Shangluo Central Hospital, Shangluo, Shanxi, China

Abstract. – OBJECTIVE: Long noncoding RNAs (lncRNAs) are important regulators involved in a variety of cancer development. However, the role of Linc00210 in non-small cell lung cancer (NSCLC) remains unknown. This study aims to investigate the clinical value of Linc00210 in NSCLC patients and the biological functions of Linc00210 in NSCLC.

PATIENTS AND METHODS: Gene expression in NSCLC tissues and cell lines was detected using qRT-PCR or Western blot. 3-(4,5-dimethyl-2-thiazolyl)-2,5-diphenyl-2-H-tetrazolium bromide (MTT) and colony formation assays were conducted to evaluate the effect of Linc00210 on NSCLC cell proliferation. Transwell assay and annexin V-Fluorescein 5-isothiocyanate (FITC)/ Propidium Iodide (PI) were done to analyze the effect of Linc00210 on cancer cell invasion and apoptosis, respectively. Luciferase reporter assay and RIP assay were performed to determine the target of Linc00210 and miR-16-5p. Besides, these assays were used to determine reciprocally inhibition of each other-controlled NSCLC cell behaviors. *In vivo* tumorigenesis experiments were applied to exhibit subcutaneous tumor growth.

RESULTS: Linc0021 was highly expressed in NSCLC tissues and cell lines. Knockdown of Linc00210 inhibited cancer cell proliferation and invasion, and increased cell apoptosis, and regulated the expression of Cyclin A1, proliferating cell nuclear antigen (PCNA), E-cadherin, N-cadherin, Bax, and Bcl-2 in NSCLC cells. Further data showed Linc00210 bound to and directly modulated the miR-16-5p levels. Impressively, overexpression of miR-16-5p suppressed NSCLC cell proliferation and invasion, but increased cell apoptosis, and these behaviors could be overturned by overexpression of Linc00210 in vitro and *in vivo*. Finally, Linc00210 and miR-16-5p cooperatively controlled expression of protein tyrosine kinase 2 (PTK2), a miR-16-5p target.

CONCLUSIONS: Linc00210/miR-16-5p/PTK2 signaling suggests a promising novel strategy for anti-NSCLC therapy.

Key Words:
Linc00210, MiR-16-5p, PTK2, Non-small cell lung cancer, Xenografts.

Introduction

Lung cancer has become the leading cause of cancer deaths worldwide[1,2]. It includes two types of cancers, small cell and non-small cell lung cancers (NSCLCs) and squamous cell carcinoma of lung cancer, and NSCLCs is the chief type of human lung cancer[3,4]. The 5-year survival rate of MSCLC patients is about 15% largely owing to its recurrence and poor therapeutic plans[3]. During lung cancer initiation and development, abnormal cancer cell behaviors including cell growth, invasion, migration, and apoptosis. These cell behaviors are coupled with gene mutation and dysregulation. However, these dysfunctions are not fully interpreted. Together, it is essential to investigate the underlying molecular mechanisms of NSCLC progression, and to explore the novel therapeutic targets for NSCLC treatment.

Long noncoding RNAs (lncRNAs) are defined as nonprotein-coding RNAs, which are longer than 200 nucleotides[5]. LncRNAs have functioned in various cancers[6-8]. We take some familiar lncRNAs for example. HOX transcript antisense RNA (HOTAIR) increases lung cancer cell invasion and motility[9]. Inhibition of rhophilin, Rho GTPase binding protein 1 antisense RNA 1 (RHPN1-AS1) triggers gefitinib resistance of NSCLC cancer via regulating MicroRNA (miR)-299-3p/ TNFAF12[10]. Maternally expressed 3 (MEG3) inhibits NSCLC cell proliferation and promotes p53-induced apoptosis[11]. Actin filament associated protein 1 antisense RNA 1 (AFAP1-AS1) promotes NSCLC tumorigenesis by suppressing p21 expression[12,13]. In this study, we selected Linc00210

Corresponding Author: Caoni Li, MD; e-mail: natsci2019@yeah.net

as a key molecular by checking the records of lncRNA in Lnc2Cancer database (http://www.bio-bigdata.net/lnc2cancer/search_quick_res.jsp?-searchname=linc00210), and its functions and its pathogenic mechanism in NSCLC remain unclear. According to the previous studies, Linc00210 is a positive regulator of liver tumorigenesis, and it interacts with catenin beta interacting protein 1 (CTNNBIP1) resulting in activation of WNT/β-catenin signaling[14]. Linc00210 sponging miR-195-5p to enhance the malignancy of thyroid cancer cells by activating insulin like growth factor 1 receptor (IGF1R)-mediated phosphatidylinositol 3-kinase/serine/threonine kinase (PI3K/Akt) signaling[15]. Then, Linc00210 also promotes nasopharyngeal carcinoma tumorigenesis by activating miR-328-5p-mediated repression notch receptor 3 (NOTCH3) signaling[16]. Consequently, we can conclude that Linc0021 also might be an oncogene in NSCLC development. Thus, we investigated the biological function and the pathogenic mechanism of Linc00210 in NSCLC, offering promising targets for therapeutic treatment of NSCLC.

Interaction with microRNAs (miRNAs) presents a common manner for lncRNAs exerting their functions in disease[10,15,16]. Herein, we found that Linc00210 mainly distributed in cytoplasm, suggesting that Linc00210 might show its oncogenic activity by interacting with miRNAs in NSCLC. Using DIANA tools (http://carolina.imis.athena-innovation.gr/diana_tools/web/index.php?r=lncbasev2/index) to predict the binding miRNAs of Linc00210. For the first time, we observed that Linc002210 may serve as a molecular sponge of miR-16-5p, which participates in cancer development including lung cancer[17,18]. For instance, miR-16-5p, regulated by lncRNA plasmacytoma variant translocation 1 (PVT1), represses cell proliferation, invasion and epithelial-mesenchymal transition in renal cell carcinoma[19]. MiR-16-5p, sponged by ANK repeat and PH domain-containing protein 2 antisense RNA 1 (AGAP2-AS1), inhibits cell proliferation and metastasis in hepatocellular carcinoma[20,21]. Additionally, miR-16-5p, regulated by MIR205 host gene (MIR205HG), significantly inhibits tumor growth and progression of cervical cancer[22]. MiR-16-5p-carried exosomes can suppress progression of colorectal cancer by targeting intergrin-2 (ITG2)[23]. *In vitro* and *in vivo* experiments demonstrate that miR-16-5p serves as a tumor suppressor of chordoma cell proliferation, invasion and metastasis by targeting Smad3[24]. Overexpression of miR-16-5p enhances radio-sensitivity by regulating Cyclin D1-mediated signaling in prostate cancer[25]. MiR-16-5p-SMAD family member 3 (SMAD3) signaling is involved in melatonin-induced inhibition of cell proliferation of gastric cancer[26], and meanwhile, miR-16-5p-vascular endothelial growth factor (VEGF)-A axis is involved in angiogenesis of chondrosarcoma[27]. MiR-16-5p also acts as a tumor suppressor in breast cancer and glioma[28,29]. Impressively, miR-16-5p could significantly protect lipopolysaccharide (LPS)-stimulated A549 cell injury by binding C-X-C Motif chemokine receptor 3 (CXCR3), a novel target for targeted treatment of lung cancer[30]. Consequently, we assume that the oncogenic lncRNA Linc00210 may exhibit its functions by sponging miR-16-5p, a promising tumor suppressor, in lung cancer development.

As we know, miRNAs present a series of highly conserved small nonprotein-coding RNAs that are able to enhance the degradation of messenger RNAs or to suppress their translation largely by binding to 3′-untranslated regions (3′-UTRs) of mRNAs[31]. In our study, we observed that PTK2, a common oncogene, might be a direct target of miR-16-5p predicted by using TargetScan database, and PTK2 expression can be synergistically modulated by miR-16-5p and Linc00210.

In this study, we investigated the role of Linc00210/miR-16-5p/PTK2 signaling in NSCLC progression. Our data reported that Linc00210 is significantly increased in lung cancer tissues. Then, Linc00210 promotes cell proliferation, invasion, and inhibits cell apoptosis of Calu-3 and H1299 cell lines through regulating miR-16-5p/PTK2 signaling *in vitro* and *in vivo*.

Patients and Methods

Clinic Sample Collection

Forty human lung cancer tissues and their adjacent non-cancerous tissues were obtained from patients with lung cancer at the Shangluo Central Hospital, Shangluo, Shanxi, 726000, China. The collected tissues have not been subjected to to radiotherapy or chemotherapy. The participants all have signed an informed consent form. The diagnoses of patients with lung cancer were verified by pathologists. The clinic sample collection was carried our following the approved guidelines, and this investigation was approved by the Ethics Committee of Shangluo Central Hospital (SLCH 2016-0018).

Cell Culture

The used cell lines were purchased from the Cell Bank of the Chinese Academy of Science (Shanghai, China).

BEAS-2B, A549, Calu-3, H1299, SPCA-1, and PC-9 cells were cultured in Dulbecco's Modified Eagle's Medium (DMEM; GIBCO, Carlsbad, CA, USA) supplemented with 10% fetal bovine serum (GIBCO; Carlsbad, CA, USA) and 100 U/ml penicillin and 100 μg/ml streptomycin (GIBCO, Carlsbad, CA, USA). They were incubated in a 37°C humidified atmosphere containing 5% CO_2.

Plasmids, Small Interfering RNA Sequences, and Lenti-Viruses

All the plasmids, small interfering RNA (siRNA), and lenti-viruses were designed and synthesized by GenePharma (Shanghai, China). Linc00210-small interfering RNA (siRNA) (si-Linc00210) was 5′-GCA CUG AAG UUC UGU AAA UUU-3′, and this siRNA was also expressed by sh-Linc00210, and the control siRNA (si-NC) was 5′-AGA UCG ACG UGG CGU AAU CCA-3′. Then, the si-Linc00210 and full length of LINC-00210 (Ensembl Transcript ID: ENST00000431637) were constructed into an empty vector named pcDNA3.1 (+), and they are also constructed into lenti-virus used for animal experiments. At the same time, the Mock is 5′-UCU CCG AAC GUG UCA CGU-3′, and miR-16-5p mimic is 5′-UAG CAG CAC GUA AAU AUU GGC G-3′, and miR-16-5p inhibitor is 5′-CGC CAA TAA AGC TGC TGC TA-3′. On the other hand, full length of Linc00210 and 3′UTR of PTK2 as well as their mutants, were inserted into Luciferase reporter plasmid (pmirGLO) (Promega, Madison, WI, USA). The plasmids and oligonucleotides were transfected into lung cancer cells using the agent Lipofectamine 3000 (Thermo Fisher Scientific, Waltham, MA, USA) according to its manufacturer's instructions.

Hematoxylin and Eosin (H&E) Staining

Clinic lung cancer tissues and their adjacent normal tissues were firstly fixed in 4% paraformaldehyde. Then, they were embedded, and sectioned. Finally, they were stained with hematoxylin and eosin (H&E) as previously described[32]. The H&E staining agents were bought from Thermo Fisher Scientific (Waltham, MA, USA).

Quantitative Real-Time Polymerase Chain Reaction (qRT-PCR)

Total cellular RNAs of tissues or cell lines were extracted using TRIzol method following the manufacturer's instructions (Thermo Fisher Scientific, Waltham, MA, USA). After isolation of RNAs, 500 ng RNA was synthesized to complementary DNA (cDNA) using a PrimeScript RT Kit (Cat. no. #RR037A v.0610, TaKaRa, Dalian, China) according to the manufacturer's instructions. The RNA expression was analyzed using SYBR Premix Ex Taq II and Perfect Real Time (Cat. no. #DRR081A, TaKaRa, Dalian, China). Levels of Linc00210, miR-16-5p, and PTK2, Cyclin A1, PCNA, E-cadherin, N-cadherin, Bax, and Bcl-2 were normalized to the expression levels of 18S RNA, U6, and glyceraldehyde-3-phosphate dehydrogenase (GAPDH), respectively. Gene expression was calculated according to the $2^{-\Delta\Delta Ct}$ method. qRT-PCR primers were listed in Table I.

Table I. Sequences of used primers in this study.

Gene name	Primer forward	Primer Reverse
Linc00210	5′-AAC ACG TTA GCG GGT TCT CA-3′	5′-TCA AAA ACC ACC GAG GGA GG-3′
18S RNA	5′-CGT TCT TAG TTG GTG GAG CG-3′,	5′-CCG GAC ATC TAA GGG CAT CA-3′
PTK2	5′-CAG GGT CCG ATT GGA AAC CA-3′	5′-CTG AAG CTT GAC ACC CTC GT-3′
GAPDH	5′-CAC CCA CTC CTC CAC CTT TG-3′	5′-CCA CCA CCC TGT TGC TGT AG-3′
Cyclin A1	5′-TCA CTT GGG ATG GAG ACC G-3′	5′-GCT GCT GCT GGA AGA CGA AA-3′
PCNA	5′-CTC TTC CCT TAC GCA AGT CTC A-3′	5′-GTG CCT CCA ACA CCT TCT TG-3′
N-cadherin	5′-TGC ATG AAG GAC AGC CTC TT-3′	5′-TGG GTC TCT TTG TCT TGG GC-3′
E-cadherin	5′-ATG CTG ATG CCC CCA ATA CC-3′	5′-TGC CAT CGT TGT TCA CTG GA-3′
Bax	5′-GGG TTG TCG CCC TTT TCT AC-3′	5′-AGT CGC TTC AGT GAC TCG G-3′
Bcl-2	5′-CTT TGA GTT CGG TGG GGT CA-3′	5′-GGG CCG TAC AGT TCC ACA AA-3′
miR-16-5p	5′-UAG CAG CAC GUA AAU A-3′	5′-GTG CAG GGT CCG AGG T-3′
U6	5′-AAC GAG ACG ACG ACA GAC-3′	5′-GCA AAT TCG TGA AGC GTT CCA TA-3′
miR-16-5p RT	5′-GTC GTA TCC AGT GCA GGG TCC GAG GTA TTC GCA CTG GAT CGC CAA-3′	
U6 RT	5′-GTC GTA TCC AGT GCA GGG TCC GAG GTA TTC GCA CTG GAT ACG ACA AAT ATG-3′	

Western Blot

The total protein of lung tissues or cell lines was extracted by using radioimmunoprecipitation assay lysis buffer (RIPA buffer) (Cat. no. # P0013C, Beyotime, Shanghai, China). After lysing for 30 min at ice, the samples were centrifuged for 15 min at 12,000 rpm. The concentration of total protein was quantified by bicinchoninic acid (BCA) Protein Assay Kit (Cat. no. # P0012, Beyotime, Shanghai, China). The supernatant of each sample was placed in a new Eppendorf (EP) tube, and it was boiled with sodium dodecyl benzene sulfonate sodium dodecyl benzene sulfonate (SDS) loading buffer for 10 min. Then, 40 μg protein was subjected to polyacrylamide gel electrophoresis, and the separated protein was transferred onto a polyvinylidene difluoride (PVDF) membrane (Cat. no. # 1704157, Bio-Rad Laboratories, Hercules, CA, USA). Next, protein carried PVDF membrane was blocked by 5% skimmed milk for 1 h, and the membrane was incubated with the primary antibody at 4°C overnight, and it was covered with the secondary antibody at 4°C for 2 h. After capturing on an optical luminescence instrument (Cat. No. #Tanon 4600SF, Tanon, Shanghai, China), the optical density of protein band was analyzed using Image J software (Media Cybernetics, Bethesda, MD, USA). A variety of antibodies were used in this study including Cyclin A1 (Cat. no. #4656, Cell Signal Technology, Danvers, MA, USA), PCNA (Cat. no. #13110, Cell Signal Technology, Danvers, MA, USA), E-cadherin (Cat. no. #2518, Cell Signal Technology, Danvers, MA, USA), N-cadherin (Cat. no. #99377, Cell Signal Technology, Danvers, MA, USA), Bax (Cat. no. #5023, Cell Signal Technology, Danvers, MA, USA), Bcl-2 (Cat. no. #15071, Cell Signal Technology, Danvers, MA, USA), PTK2 (Cat. no. #3285, Cell Signal Technology, Danvers, MA, USA), GAPDH (Cat. no. #51332, Cell Signal Technology, Danvers, MA, USA), horseradish peroxidase (HRP)-labeled goat anti-rabbit or -mouse secondary antibody (Cat. no. # BS13278 or #BS12478, Bioworld, Minnesota Twin Cities, Hilton Minneapolis-Saint Louis Park at West End, China).

MTT Assay

We applied 3-(4,5-dimethyl-2-thiazolyl)-2,5-diphenyl-2-H-tetrazolium bromide (MTT) assay to evaluate the cell proliferation of cancer cell lines. 4×10^3 cells were planted in a 96-well plate. After transfection for 24 h, 10 μl MTT agent was added into 100 μl medium per well for 1 h at 37°C. Then, the 570 nm value was measured on a microplate reader. The MTT was bought from Thermo Fisher Scientific (Waltham, MA, USA).

Colony Formation

In this study, we also conducted colony formation assay to determine the cancer cell proliferation. First, 5×10^3 cells were seeded in a 6-well plate. After transfection for 24 h, the cells were cultured for the next 12 days. Then, all colonies were fixed with ethanol and they were stained with 0.2% crystal violet for 2 h. They were captured under a light microscope Carl Zeiss (Axio Observer A1, Jena, Germany). The use plates and agents were from Thermo Fisher Scientific (Waltham, MA, USA).

Transwell Assay

In this experiment, 2×10^5 cells were firstly transfected with plasmids and siRNAs for 36 h. Then, they were planted in the upper chamber with Matrigel-coated membrane (Cat. no. # 354230, Thermo Fisher Scientific, Waltham, MA, USA) and incubated in serum-free DMEM. The lower chamber was added with FBS-containing medium. After 24 h incubation, the invading cells in the down chamber were fixed with methanol. The invaded cells were stained with 0.2% crystal violet for 2 h. They were captured under a light microscope Carl Zeiss (Axio Observer A1, Jena, Germany). The use transwell plates and other agents were from Thermo Fisher Scientific (Waltham, MA, USA).

Annexin V-FITC/Propidium Iodide Staining

The cells were transfected with plasmids and siRNAs for 36 h. All cells were collected by using trypsin, and they were resuspended in phosphate-buffered saline (PBS). Then, these cells were stained with 5 μl FITC-annexin V and 10 μl propidium iodide (PI) (Cat. no. #C1062L, Beyotime, Shanghai, China) for 15 min in a dark room. After washing with phosphate-buffered saline (PBS), the samples were detected by a Becton Dickinson flow cytometry (Becton Dickinson, Franklin Lakes, NJ, USA), and they were labeled as apoptotic cells stained by both Annexin V-FITC and PI.

Luciferase Reporter Assay

The Luciferase reporter plasmids, wide type (WT) and mutant of pmirGLO-Linc00210 and 3'UTR of PTK2, were co-transfected with miR-

16-5p mimic and inhibitor into cancer cells. The wide type and mutant of Linc00210 and PTK2 3'UTR were synthetized and constructed into pmirGLO empty vector by Sangon (Shanghai, China). After transfection for 24 h, we harvested the cells for Luciferase activity analysis applying Dual-Luciferase Reporter Assay System (Promega, Madison, WI, USA).

Nuclear-Cytoplasmic Isolation

To determine the location of Linc00210 in cancer cells, the PARIS Kit (Cat. no. #AM1921, Life Technologies, Waltham, MA, USA) was applied. We successfully isolated nuclear and cytoplasmic and nuclear fractions. GAPDH and U6 were considered as the cytoplasmic endogenous control and nuclear endogenous control, respectively.

RNA-Chromatin Immunoprecipitation (RIP)

RIP was applied to explore the potential endogenous binding between Linc00210 and miR-16-5p using Magna RIP™ RNA-Binding Protein Immuno-Precipitation Kit (Millipore, Billerica, MA, USA). The primary antibody against Ago- 2 (Cat. no. SAB4301150, Sigma, Aldrich, St. Louis, MO, USA) or IgG (Cat. no. I4131, Sigma-Aldrich, St. Louis, MO, USA) was added into lysate for RIP assay. RNA was extracted using TRIzol agent, and the indicated RNA content was measured by qRT-PCR as described above.

Nude Mice Experiments

To determine the effect of Linc00210 and miR-16-5p on cancer cell behaviors, we plated transfected cells into 4-week old nude mice (Beijing Vital River Laboratory Animal Technology, Beijing, China) to observe the tumor growth. This animal experiment was approved by the Ethics Committee of Shangluo Central Hospital (SLCH 2016-0018) (Shangluo City, Shanxi, China). We declared that all animals were given proper care according to the relevant guidelines and regulations. All mice were housed in a specific pathogen-free room, belonging to the Shangluo Central Hospital, at 25-26°C. The cancer cell line (Calu-3) was collected after 72 h transfection with Linc00210, miR-16-5p, and PTK2. Then, these cells were resuspended into PBS and they were subcutaneously injected into mice (2 for each group). During the whole process, the mice were anaesthetized with 0.3% chloral hydrate. Finally, the mice were sacrificed by cervical vertebra dislocation on the last day to harvest the tumors. Tumor volume and weight were recorded at the indicative time. Tumor volume was confirmed according to the formula[33]: volume = (longest diameter × shortest diameter^2)/2.

Statistical Analysis

The results are expressed as mean ± standard deviation (SD). The GraphPad Prism 5 Software (La Jolla, CA, USA) was used to analyze all the data. The means of two groups were compared using a two-tailed Student's *t*-test, and multi-group comparisons were performed using a Chi-square test. A p-value<0.05 was statistically significant. All the experiments were independently conducted in triplicate.

Results

Linc00210 is Highly Expressed in Lung Cancer Tissues and Cancer Cells

First, the pathological changes of lung cancer tissues were detected by H&E staining. The data showed that abnormal growth and distribution of kinds of cells appeared in cancer tissues (Figure 1A). To investigate the role of LINC00219 in NSCLC tumorigenesis, qRT-PCR was performed to evaluate the Linc00210 levels in 40 paired lung cancer tissues and adjacent non-tumor tissues. As exhibited in Figure 1B, we found that Linc00210 was significantly overexpressed in lung cancer tissues compared with the adjacent normal lung tissues (Figure 1B). Meanwhile, qRT-PCR was conducted to detect the expression of Linc00210 in lung cancer cells A549, Calu-3, SPCA-1, PC-9, and H1299, compared with normal lung cell line BEAS-2B (Figure 1C).

Knockdown of Linc00210 Affects Cancer Cell Proliferation, Invasion, and Apoptosis

To explore the function of Linc00210 in lung cancer, we knocked down Linc00210 with si-Linc00210 in Calu-3 and H1299 cells, and qRT-PCR analysis demonstrated that Linc00210 level was significantly decreased in these cancer cell lines (Figure 2A, B). Then, MTT assay was conducted to determine the effect of Linc00210 on proliferation, and knockdown of Linc00210 was able to suppress the ability of cell proliferation in both Calu-3 and H1299 cells (Figure 2C, D). Sim-

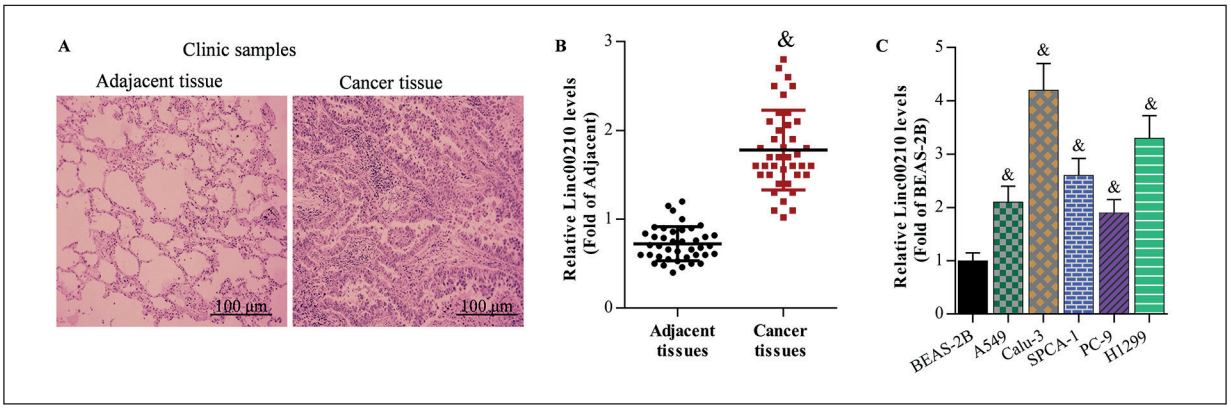

Figure 1. Linc00210 is elevated in lung cancer tissues and cancer cells. **A**, H&E staining analysis of lung clinic tissues at 10×20× magnification. **B**, The level of Linc00210 in NSCLC tissues (n=40) was determined by qRT-PCR; &$p<0.01$, compared with adjacent non-tumour tissues. **C**, The level of Linc00210 in cancer cells was detected by qRT-PCR; &$p<0.01$, compared with BEAS-2B (normal lung cell lines). All the data are presented as the mean ± SD of three independent experiments, each performed in triplicate.

ilarly, interfering Linc00210 expression significantly reduced colony formation of cancer cells (Figure 2E, F). We also found that knockdown of Linc00210 significantly inhibited expression of cell growth-associated genes such as Cyclin A1 and PCNA (Figure 2G).

Transwell assay was performed to investigate whether Linc00210 plays an important role in modulating the invasion of lung cancer cells. The data demonstrated that silencing of Linc00210 can significantly inhibit the invading ability of Calu-3 and H1299 cells (Figure 2H, I). Correspondingly, downregulation of Linc00210 could elevate E-cadherin expression and reduce N-cadherin level (Figure 2J).

Finally, annexin V-FITC/PI analysis showed that knockdown of Linc00210 could significantly increase cell apoptosis in Calu-3 and H1299 cells (Figure 2K, L). Consistently, qRT-PCR analysis showed that downregulation of Linc00210 markedly enhanced Bax expression and inhibited Bcl-2 expression (Figure 2M). These results suggest that Linc00210 could promote the growth and invasion, and it could suppress cell apoptosis of lung cancer.

Linc00210 Functions as a Sponge for MiR-16-5p

Cytoplasmic lncRNAs have been served as competing endogenous RNAs to sponge mRNAs. Linc00210 has been reported that it can function as a competing endogenous RNA (ceRNA) to regulate the progression of several types of cancer. Consistently, our results told that Linc00210 was mainly located in cytoplasm rather than in nucleus (Figure 3A). Accordingly, we suspected that Linc00210 may be a regulator of NSCLC development in a ceRNA manner. Using DIANA tools, we identified the potential binding sites of miR-16-5p on Linc00210 (Figure 3B). Further data demonstrated that miR-16-5p was dramatically decreased in lung cancer tissues and lung cancer cell lines (Figure 3C, D), suggesting that miR-16-5p might be regulated by Linc00210. To further confirm whether Linc00210 may sponge miR-16-5p, we carried out a series of experiments. At the beginning, knockdown of Linc00210 significantly downregulated miR-16-5p expression in Calu-3 and H1299 cells (Figure 3E), and miR-16-5p also negatively controlled Linc00210 expression (Figure 3F). Moreover, miR-16-5p negatively regulated Luciferase activity of Linc00210-WT rather than Linc00210-Mutant evidenced by Luciferase reporter assay (Figure 3G). Finally, both Linc00210 and miR-16-5p were enriched by anti-Ago2-mediated RNA immunoprecipitation (RIP) in Calu-3 and H1299 cells (Figure 3H). Taken together, these findings showed that Linc00210 could be a molecular sponge of miR-16-5p in NSCLC progression.

MiR-16-5p is a Tumor Suppressor in NSCLC Cells and its Activity is Counteracted by Linc00210 Overexpression

In our study, miR-16-5p was decreased in NSCLC tissues and cell lines, and miR-16-5p expression can be suppressed by overexpression of Linc00210, which was proved to be an oncogene in NSCLC development by our data. These findings suggested that miR-16-5p may be a tumor

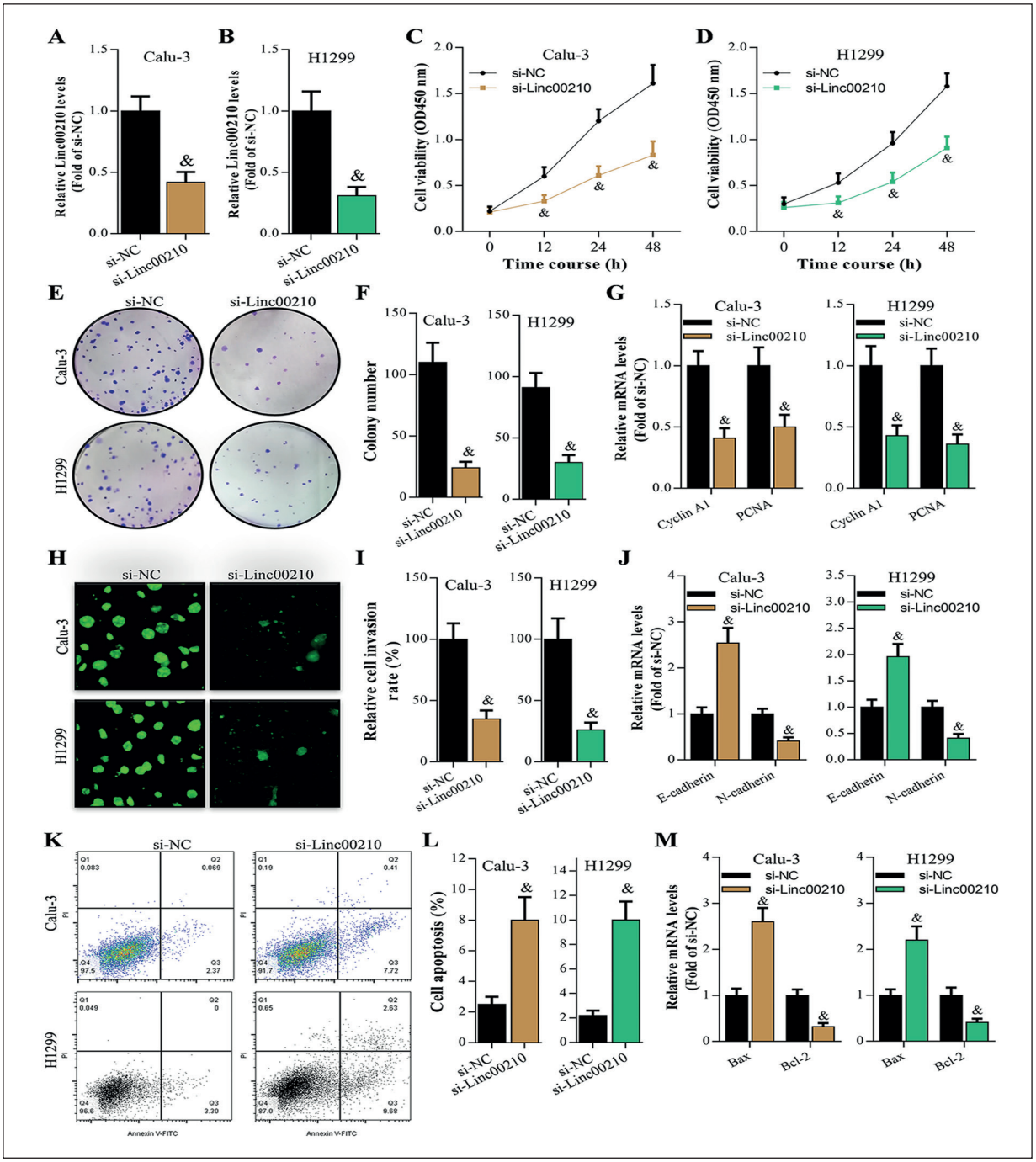

Figure 2. Knockdown of Linc00210 inhibits cell proliferation and invasion and increases cell apoptosis in vitro. **A**, **B**, The expression of Linc00210 in NSCLC cells transfected with si-Linc00210 or si-NC was analyzed by qRT-PCR; &p<0.01, compared with si-NC. **C**, **D**, CCK-8 assays showed that knockdown of Linc00210 inhibited cancer cell growth; &p<0.01, compared with si-NC. **E**, **F**, Colony formation assays showed that knockdown of Linc00210 suppressed cancer cell colony formation at 1×1× magnification; &p<0.01, compared with si-NC. **G**, qRT-PCR analysis showed that downregulation of Linc00210 decreased expression of cell growth-associated genes including Cyclin A1 and PCNA; &p<0.01, compared with si-NC. **H**, **I**, Transwell assays showed that knockdown of Linc00210 suppressed cancer cell migration at 10×40× magnification; &p<0.01, compared with si-NC. **J**, qRT-PCR analysis showed that interfering Linc00210 reduced expression of cell migration-associated genes including E-caderin and N-caderin; &p<0.01, compared with si-NC. **K**, **L**, Annexin V-FITC/PI analysis exhibited that knockdown of Linc00210 enhanced cancer cell apoptosis; &p<0.01, compared with si-NC. **M**, qRT-PCR analysis showed that silencing of Linc00210 elevated expression of cell apoptosis-related genes including Bax and Bcl-2; &p<0.01, compared with si-NC. All the data are presented as the mean ± SD of three independent experiments, each performed in triplicate.

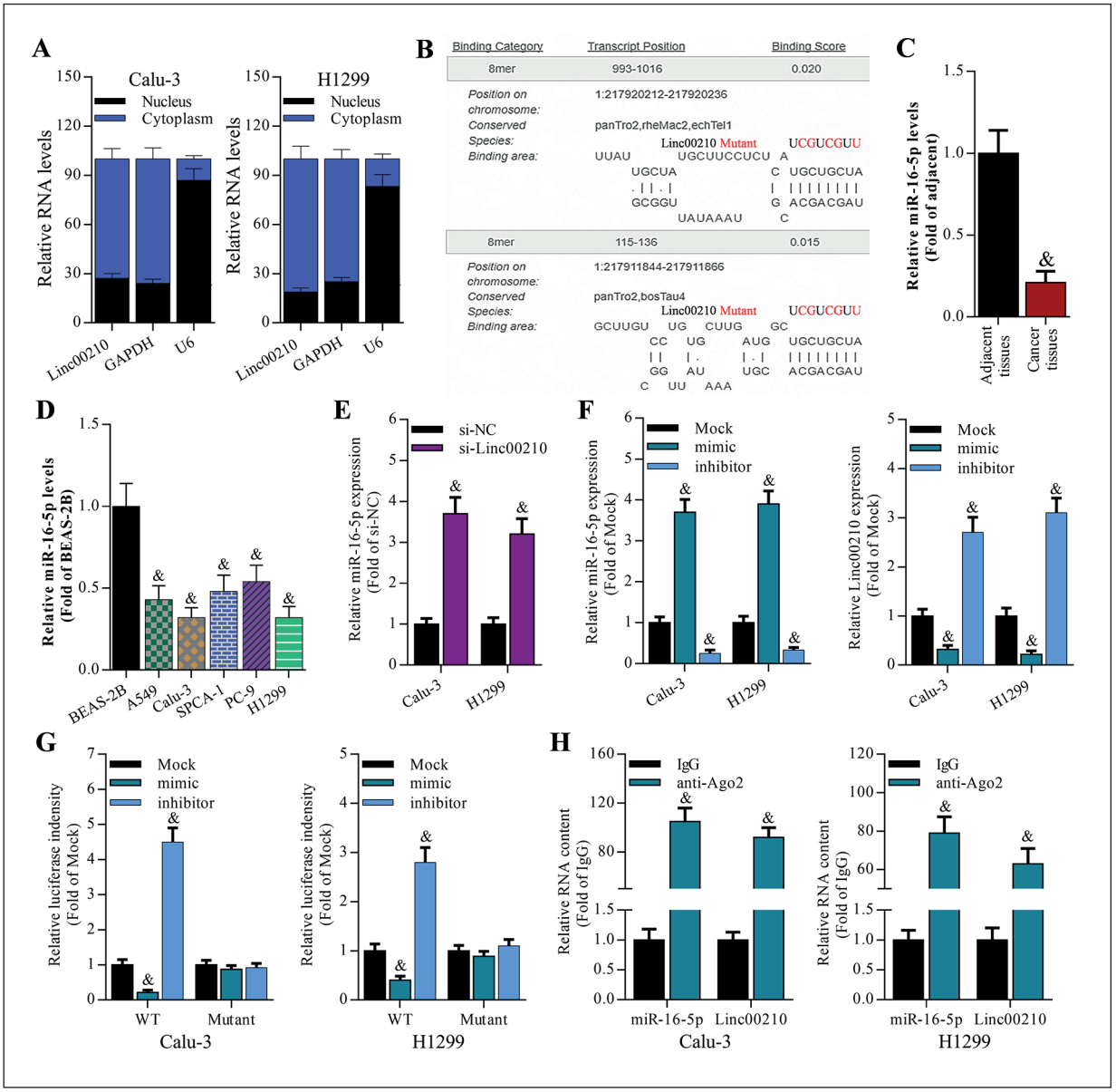

Figure 3. The interaction of Linc00210 with miR-16-5p. **A**, The location of Linc00210 in cytoplasm and nucleus of cancer cells were assessed by qRT-PCR. **B**, The putative binding sites of miR-16-5p on Linc00210 were predicted by DIANA tools. **C**, The level of miR-16-5p in NSCLC tissues (n=40) was determined by qRT-PCR; &p<0.01, compared with adjacent non-tumor tissues. **D**, The level of miR-16-5p in cancer cells was analyzed by qRT-PCR; &p<0.01, compared with BEAS-2B. **E**, qRT-PCR analysis showed that knockdown of Linc00210 upregulated miR-16-5p expression; &p<0.01, compared with si-NC. **F**, qRT-PCR analysis indicated that miR-16-5p affected Linc00210 expression in cancer cells; &p<0.01, compared with Mock. **G**, Luciferase assay showed that miR-16-5p regulates the Luciferase activity of Linc00210-WT, rather than that of Linc00210-mutant; &p<0.01, compared with Mock. **H**, RIP assay showed that both Linc00210 and miR-16-5p were enriched in the Ago-2 precipitate compared with IgG; &p<0.01, compared with anti-IgG. All the data are presented as the mean ± SD of three independent experiments, each performed in triplicate.

suppressor and its activity can be inhibited by overexpression of Linc00210. Colony formation assays and transwell assays showed that miR-16-5p overexpression suppressed the growth of NSCLC cells but notably, this was reversed by concomitant overexpression of Linc00210 (Figure 4A, B). Meanwhile, miR-16-5p overexpression significantly elevated cell apoptosis in Calu-3 and H1299 cells while this activity can be overturned by Linc00210 overexpression (Figure 3C).

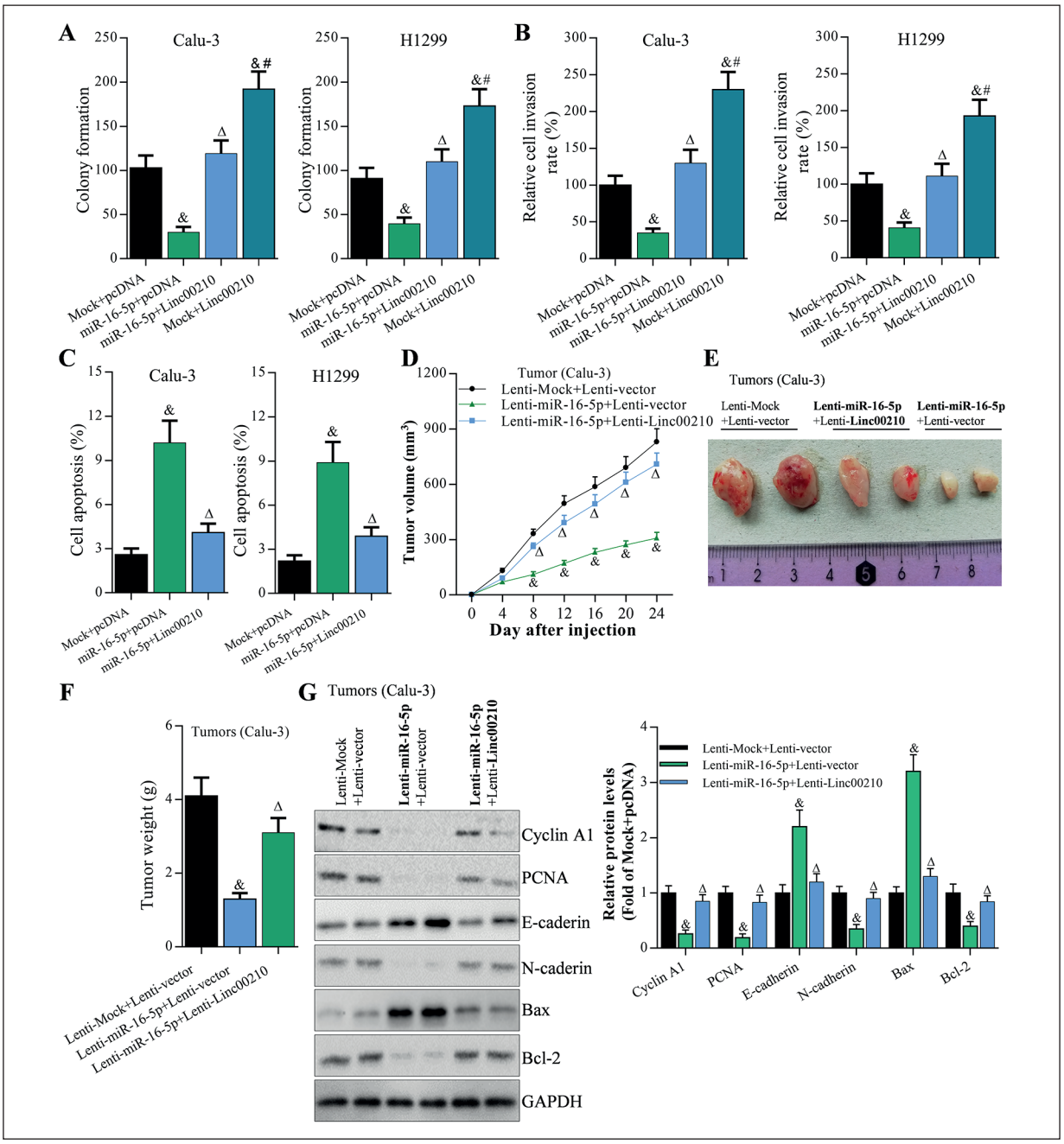

Figure 4. Linc00210 reversed miR-16-5p-regulated cancer cell proliferation, invasion, and apoptosis *in vitro* and *in vivo* by sponging miR-16-5p. **A**, Colony formation assays showed that overexpression of Linc00210 reversed miR-16-5p-induced inhibition of colony formation of Calu-3 and H1299 cells; &p<0.01, compared with Mock+pcDNA, Δp<0.01, compared with miR-16-5p+pcDNA, #p<0.01, compared with miR-16-5p+Linc00210. **B**, Transwell assays showed that overexpression of Linc00210 blocks miR-16-5p-mediated inhibition of cell migration of Calu-3 and H1299 cells; &p<0.01, compared with Mock+pcDNA, Δp<0.01, compared with miR-16-5p+pcDNA, #p<0.01, compared with miR-16-5p+Linc00210. **C**, Annexin V-FITC analysis showed that overexpression of Linc00210 reversed miR-16-5p-induced increase of apoptosis of Calu-3 and H1299 cells; &p<0.01, compared with Mock+pcDNA, Δp<0.01, compared with miR-16-5p+pcDNA. **D**, Overexpression of Linc00210 partly neutralized miR-16-5p-mediated suppression of tumor growth in a mouse xenograft model; &p<0.01, compared with Lenti-Mock+Lenti-vector, Δp<0.01, compared with Lenti-miR-16-5p+Lenti-vecctor. **E**, The tumors formed in nude mice on the 24th day. **F**, The tumor weight in nude mice on the 24th day; &p<0.01, compared with Lenti-Mock+Lenti-vector, Δp<0.01, compared with Lenti-miR-16-5p+Lenti-vecctor. **G**, Western blot analysis of gene expression in the tumor xenografts, and the optical density was analyzed using Image J software, &p<0.01, compared with Lenti-Mock+Lenti-vector, Δp<0.01, compared with Lenti-miR-16-5p+Lenti-vcctor. All the results are presented as the mean ± SD of three independent experiments, each performed in triplicate.

To further determine reciprocal regulation between miR-16-5p and Linc00210 in NSCLC cells, we conducted *in vivo* experiments in nude mice. Impressively, the data proved that miR-16-5p overexpression could significantly inhibit tumor growth, ant this inhibiting effect can be counteracted by Linc00210 overexpression (Figure 4D, E, F). In accordance with its tumor-suppressing effects, miR-16-5p overexpression significantly downregulated Cyclin A1, PCNA, N-cadherin, and Bcl-2, and however, miR-16-5p upregulated E-cadherin and Bax in tumors (Figure 4G). Then, miR-16-5p-mediated expression of genes can be reversed by overexpression of Linc00210 (Figure 4G). These findings suggest that Linc00210 and miR-19-5p act reciprocally as an oncogene and a suppressor, respectively, in NSCLC cells.

PTK2 is a Novel Target of MiR-16-5p and is Synergistically Regulated by Linc00210 and MiR-16-5p

To determine the potential mechanisms involved in Linc00210 and miR-16-5p-mediated signaling, the downstream targets of miR-16-5p were predicted by Targetscan database. The results showed that the famous regulator PTK2 was a potential target of miR-16-5p (Figure 5A). To test this predication, we carried out the Luciferase assays in which enzyme activity was driven by the 3′UTR of PTK2; either WT and mutated in the predicated miR-16-5p binding site. Calu-3 and H1299 cells were co-transfected with miR-16-5p, pcDNA-Linc00210, and pmirGLO-PTK2-3'UTR. The results showed that Luciferase activity was increased by overexpression of Linc00210 (Figure 5B, C). Nevertheless, Linc00210- or miR-16-5p-controlled Luciferase activity of PTK2 3'UTR was inhibited by miR-16-5p and Linc00210 reciprocally (Figure 5B, C). Moreover, qRT-PCR and Western blot analysis demonstrated that PTK2 mRNA and protein levels were significantly decreased by miR-16-5p overexpression, and contrarily, markedly elevated by Linc00210 overexpression (Figure 5D, E). Then, PTK2 expression, regulated by miR-16-5p and Linc00210, could be limited reciprocally. Thus, Linc00210 and miR-16-5p serve cooperatively to modulate PTK2 level.

Overexpression of PTK2 Partly Blocks Knockdown of Linc00210-Mediated Inhibition of Tumor Growth

To determine whether PTK2 is required for functions of Linc00210, we overexpressed PTK2 and knocked down Linc00210 expression in calu-3 cells. The *in vivo* experiments showed that interfering Linc00210 inhibited tumor growth indicated by tumor volume and tumor weight (Figure 6A, B, C). Moreover, overexpression of PTK2 partly reversed interfering Linc00210-mediated inhibition of tumor growth by regulating expression of a series of genes, which were involved in apoptosis, proliferation, and invasion (Figure 6A, B, C, D).

Discussion

Lung cancer has considered as the chief reason of cancer deaths worldwide[1,2]. The 5-year survival rate of NSCLC patients is about 15% which remains to be improved[3]. Recently, increasing lncRNAs were found to be involved in initiation or further progression of a variety of diseases including NSCLC. LncRNA RHPN1-AS1, MEG3, and AFAP1-AS1 all participate in NSCLC development by diverse molecular mechanisms[10-13]. In this study, we selected Linc00210 as a key molecular by checking the records of lncRNA in Lnc2Cancer database (http://www.bio-bigdata.net/lnc2cancer/search_quick_res.jsp?searchname=linc00210). According to the previous studies, Linc00210 can advance the liver tumorigenesis by interacting with catenin beta interacting protein 1 (CTNNBIP1) leading to activation of WNT/β-catenin pathway[14]. Linc00210 has been reported as an oncogene of thyroid cancer by sponging for miR-16-5p and activating Insulin-like growth factor 1 receptor (IGF1R)-controlled PI3K/Akt pathway[15]. Similarly, Linc00210, as a molecular sponge of miR-16-5p, increases tumorigenesis of nasopharyngeal carcinoma by activating notch receptor 3 (NOTCH3) pathway[16]. Nevertheless, the role of Linc00210 remains unclear. Subsequently, we investigated the biological molecular mechanisms of Linc00210 in NSCLC cells for the first time. In accordance with these previous findings, we found that Linc00210 was upregulated in lung cancer tissues and cancer cells, suggesting that Linc00210 also functions as an oncogene in NSCLC. Impressively, *in vitro* and *in vivo* experiments in our study demonstrated that knockdown of Linc00210 inhibited cell proliferation and invasion, and elevated cell apoptosis of NSCLC cells including Calu-3 and H11299 cells. Collectively, Linc00210 functions as an oncogene during NSCLC progression.

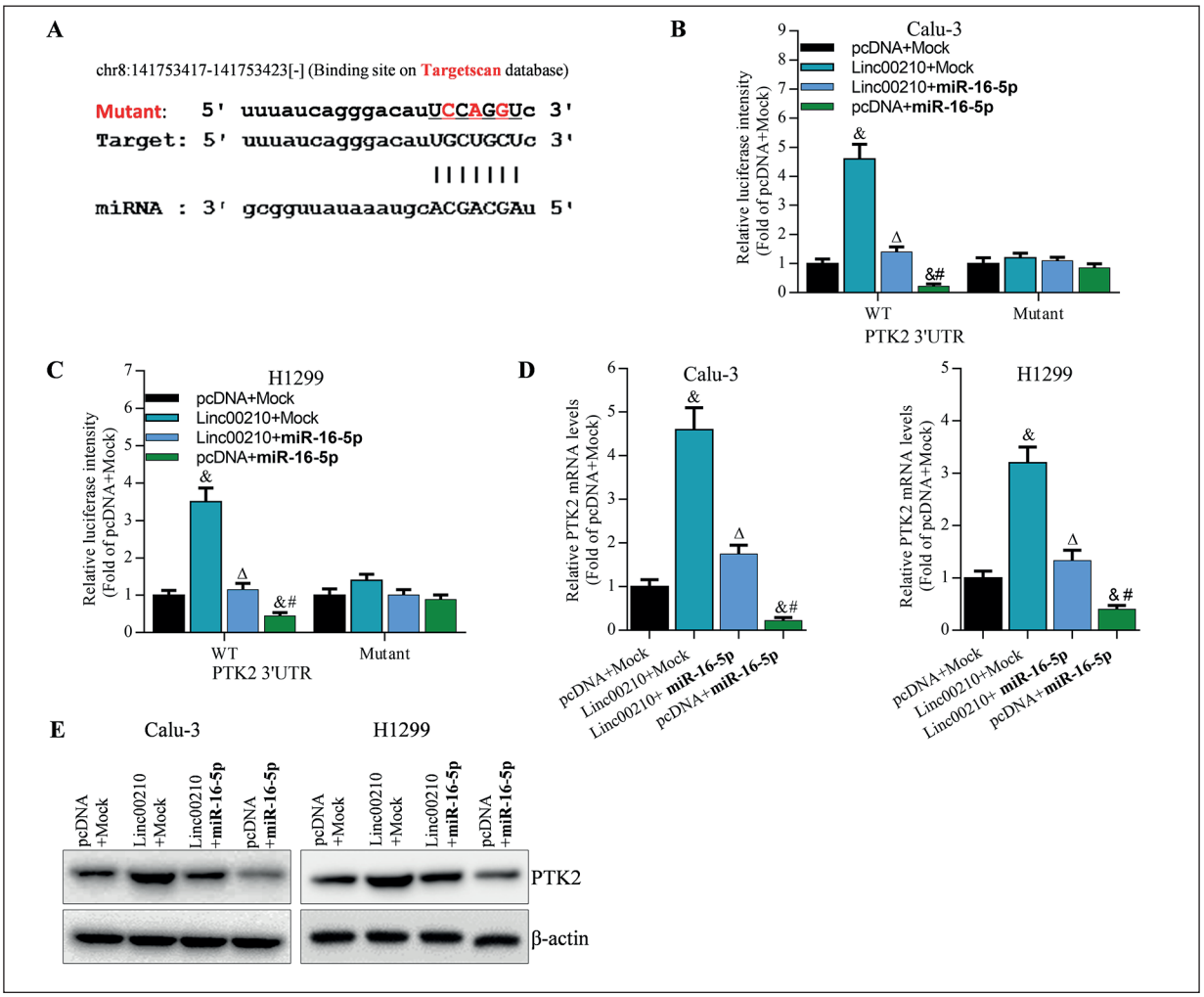

Figure 5. Linc00210 functions as a ceRNA for miR-16-5p to regulate PTK2. **A,** The putative binding sites in miR-16-5p and PTK2 sequences using PITA database. **B**, **C**, Luciferase assay showed that cooperation of miR-16-5p and LINC210 regulates the Luciferase activity of PTK2 3'UTR-WT, rather than that of PTK2 3'UTR-mutant; &p<0.01, compared with pcDNA+Mock, Δp<0.01, compared with Linc00210+Mock; #p<0.01, compared with Linc00210+miR-16-5p. **D**, qRT-PCR analysis of PTK2 mRNA expression was cooperatively regulated by miR-16-5p and Linc00210 in Calu-3 and H1299 cells; &p<0.01, compared with pcDNA+Mock, Δp<0.01, compared with Linc00210+Mock; #p<0.01, compared with Linc00210+miR-16-5p. **E**, Western blot analysis of PTK2 protein expression was cooperatively regulated by miR-16-5p and Linc00210 in Calu-3 and H1299 cells. All the data are presented as the mean ± SD of three independent experiments, each performed in triplicate.

In our study, Linc00210 was mainly located in cytoplasm, indicating that Linc00210 can serve as a sponge for miRNAs in NSCLC cells. Therefore, we predicated and demonstrated that Linc00210 may directly bind to miR-16-5p in regulation of cancer cell behaviors of NSCLC in an argonaute-2 (Ago2)/RNA-induced silencing complex (RISC)-dependent manner. Further data showed that Linc00210 performed as a molecular sponge for miR-16-5p. We found that miR-16-5p was downregulated in lung cancer tissues and cell lines, implying that miR-16-5p is a tumor suppressor. As a tumor suppressor, miR-16-5p can be sponged by lncRNA PVT1, AGAP2-AS1, and MIR205HG, and this miRNA inhibits progression of renal cell carcinoma[19], hepatocellular carcinoma[20,21], and cervical cancer, respectively[22]. MiR-16-5p-carried exosomes can suppress progression of colorectal cancer by targeting intergrin-2 (ITG2)[23]. Consistently, miR-16-5p inhibits chordoma cell proliferation, invasion, and metastasis by targeting Smad3[24]. MiR-16-5p-Smad3 axis is also involved in melatonin-mediated inhibition of gastric cancer[26]. MiR-16-5p suppresses angiogenesis of chondrosarcoma by targeting vascular endothelial growth

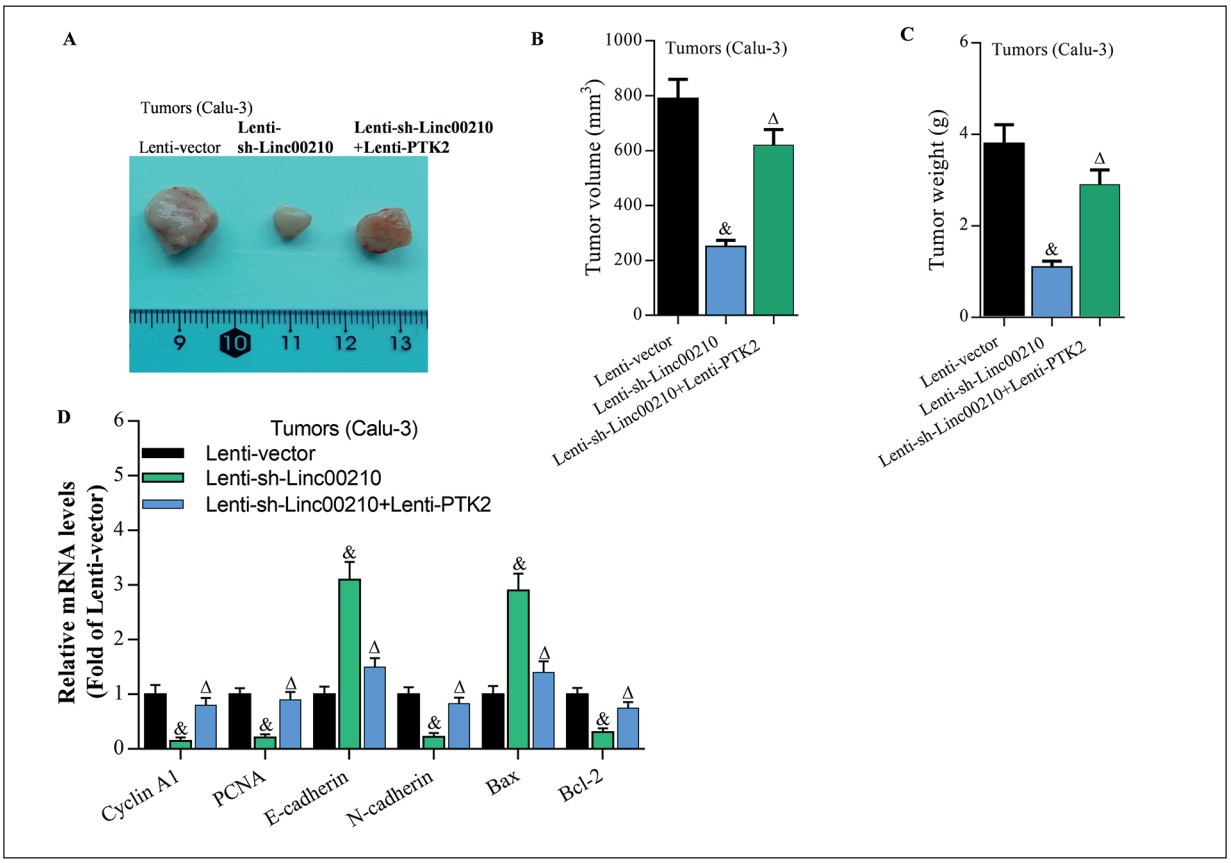

Figure 6. Overexpression of PTK2 reverses knockdown of Linc00210-mediated suppression of tumor growth in nude mice. **A**, The tumors formed in nude mice on the 24th day; &p<0.01, compared with Lenti-vector, Δp<0.01, compared with Lenti-sh-Linc00210. **B**, Overexpression of PTK2 partly blocked knockdown of Linc00210-mediated inhibition of tumor growth in a mouse xenograft model; &p<0.01, compared with Lenti-vector, Δp<0.01, compared with Lenti-sh-Linc00210. **C**, The tumor weight in nude mice on the 24th day; &p<0.01, compared with Lenti-vector, Δp<0.01, compared with Lenti-sh-Linc00210. **D**, qRT-PCR analysis of gene expression in the tumors, &p<0.01, compared with Lenti-vector, Δp<0.01, compared with Lenti-sh-Linc00210.

factor A (VEGF-A)[27]. Moreover, miR-16-5p could significantly protect LPS-induced cell injury by targeting the C-X-C Motif chemokine receptor 3 (CXCR3), suggesting that miR-16-5p might be a tumor suppressor of lung cancer. In this study, we found that miR-16-5p may be sponged by Linc00210 resulting in its downregulation in cancer cells. Overexpression of miR-16-5p inhibited Calu-3 and H1299 cell growth, colony formation, and invasion, and promoted cancer cell apoptosis. Furthermore, overexpression of miR-16-5p also inhibited gene expression such as Cyclin A1, PCNA, N-cadherin, and Bcl-2, and overexpression of miR-16-5p upregulated expression of E-cadherin and Bax *in vitro* and *in vivo*. Of note, Linc00210 and miR-16-5p may inhibit expression and functions reciprocally. Overexpression of Linc00210 reversed overexpression of miR-16-5p-regulation of cell proliferation, invasion and apoptosis *in vitro* and *in vivo*. In a word, our results are consistent with previous studies showing that miR-16-5p functions as a tumor suppressor[19-24, 26, 27, 30], and it can be sponged by Linc00210, and this study is the first research of the interaction between Linc2100 and miR-16-5p in NSCLC.

Additionally, miRNAs have been reported to exert their functions mainly by targeting 3′-UTRs of mRNAs resulting in mRNA degradation[31]. PTK2, an important oncogene, has been considered as a promising target of targeted therapy of cancers including NSCLC[34-36]. PTK2 is involved in cell proliferation, invasion, migration, and apoptosis, and other NSCLC cell behaviors, and more meaningfully, PTK2 is a positive regulator of PI3K/AKT sginalling which is a famous tum-

origenesis pathway and plays an essential role in cancer development[34-36]. Herein, PTK2 has been identified a potential target of miR-16-5p for the first time. Meanwhile, we stated the relationship between Linc00210, miR-16-5p, and PTK2. Our data showed that PTK2 can be significantly downregulated by miR-16-5p, and the PTK2 was elevated by overexpression of Linc00210, indicating that Linc00210 and miR-16-5p show their activities in NSCLC cancer partly relying on PTK2 expression. Furthermore, interaction of Linc00210 with miR-16-5p led to reciprocal inhibition of each other-regulated PTK2 expression. Finally, overexpression of PTK2 partly overturned knockdown of Linc00210-induced suppression of tumor growth, implying that PTK2 is required for Linc00210 to serve an oncogene in NSCLC. These results revealed that PTK2-involved Linc00210/miR-16-5p signaling acted an essential role in NSCLC progression *in vitro* and in *vivo*.

Conclusions

We explored in this study a novel lncRNA-mRNA-mRNA signaling in NSCLC cells. Linc00210 was upregulated in lung cancer and cancer cells, while miR-16-5p can serve as a tumor suppressor in NSCLC. Notably, reciprocal repression between Linc00210 and miR-16-5p was observed in NSCLC cancer cells. Impressively, knockdown of Linc00210 and overexpression of miR-16-5p significantly inhibited cell proliferation and invasion, and Linc00210 knockdown elevated cell apoptosis in Calu-3 and H1299 cells. Then, Linc00210 was identified as a sponge for miR-16-5p. Overexpression of Linc00210 reversed overexpression of miR-16-5p-induced cell behaviors in NSCLC *in vitro* and *in vivo*. Finally, PTK2 was a target of miR-16-5p, and PTK2 was cooperatively modulated by Linc00210 and miR-16-5p in Calu-3 and H1299 cells, and PTK2 overexpression partly overturned knockdown of Linc00210-induced repression of tumor growth in nude mice. Consequently, PTK2-involved Linc00210/miR-16-5p axis was the underlying molecular mechanism of NSCLC progression by controlling cancer cell growth, invasion, and apoptosis *in vitro* and *in vivo*. Collectively, our findings suggest that components of the Linc00210/miR-16-5p/PTK2 signaling could be promising targets for developing and improving NSCLC therapies.

Conflict of Interest

The Authors declare that they have no conflict of interests.

Ethical Approval

All applicable international, national, and/or institutional guidelines for the care and use of animals were followed. All procedures performed in our studies involving human participants were in accordance with the ethical standards of the institutional and/or national research committee and with the 1964 Helsinki Declaration and its later amendments or comparable ethical standards.

Informed Consent

Informed consent was obtained from all included participants.

Authors' Contribution

L.C.N. designed this project. P. Q. and C. Y. performed the animal experiments, and they also cultured the cell lines and conducted the cell experiments. L.C.N. and P. Q. analyzed the experimental data. L.C.N. offered discussion and suggestions. L.C.N., P. Q. and C. Y. wrote the manuscript. L.C.N. provided the financial support. All authors have reviewed this manuscript.

References

1) Siegel RL, Miller KD, Jemal A. Cancer statistics, 2017. CA Cancer J Clin 2017; 67: 7-30.
2) Chen W, Zheng R, Baade PD, Zhang S, Zeng H, Bray F, Jemal A, Yu XQ, He J. Cancer statistics in China, 2015. CA Cancer J Clin 2016; 66: 115-132.
3) Wood SL, Pernemalm M, Crosbie PA, Whetton AD. Molecular histology of lung cancer: from targets to treatments. Cancer Treat Rev 2015; 41: 361-375.
4) Boolell V, Alamgeer M, Watkins DN, Ganju V. The evolution of therapies in non-small cell lung cancer. Cancers (Basel) 2015; 7: 1815-1846.
5) Kopp F, Mendell JT. Functional classification and experimental dissection of long noncoding RNAs. Cell 2018; 172: 393-407.
6) Chang ZW, Jia YX, Zhang WJ, Song LJ, Gao M, Li MJ, Zhao RH, Li J, Zhong YL, Sun QZ, Qin YR. LncRNA-TUSC7/miR-224 affected chemotherapy resistance of esophageal squamous cell carcinoma by competitively regulating DESC1. J Exp Clin Cancer Res 2018; 37: 56.
7) Bautista RR, Gomez AO, Miranda AH, Dehesa AZ, Villarreal-Garza C, Avila-Moreno F, Arrieta O. Correction to: Long non-coding RNAs: implications in targeted diagnoses, prognosis, and improved therapeutic strategies in human non- and triple-negative breast cancer. Clin Epigenetics 2018; 10: 106.

8) Fatica A, Bozzoni I. Long non-coding RNAs: new players in cell differentiation and development. Nat Rev Genet 2014; 15: 7-21.

9) Zhao W, An Y, Liang Y, Xie XW. Role of HOTAIR long noncoding RNA in metastatic progression of lung cancer. Eur Rev Med Pharmacol Sci 2014; 18: 1930-1936.

10) Li X, Zhang X, Yang C, Cui S, Shen Q, Xu S. The lncRNA RHPN1-AS1 downregulation promotes gefitinib resistance by targeting miR-299-3p/TNFSF12 pathway in NSCLC. Cell Cycle 2018; 17: 1772-1783.

11) Lu KH, Li W, Liu XH, Sun M, Zhang ML, Wu WQ, Xie WP, Hou YY. Long non-coding RNA MEG3 inhibits NSCLC cells proliferation and induces apoptosis by affecting p53 expression. BMC Cancer 2013; 13: 461.

12) Yin D, Lu X, Su J, He X, De W, Yang J, Li W, Han L, Zhang E. Long noncoding RNA AFAP1-AS1 predicts a poor prognosis and regulates non-small cell lung cancer cell proliferation by epigenetically repressing p21 expression. Mol Cancer 2018; 17: 92.

13) Deng J, Liang Y, Liu C, He S, Wang S. The up-regulation of long non-coding RNA AFAP1-AS1 is associated with the poor prognosis of NSCLC patients. Biomed Pharmacother 2015; 75: 8-11.

14) Fu X, Zhu X, Qin F, Zhang Y, Lin J, Ding Y, Yang Z, Shang Y, Wang L, Zhang Q, Gao Q. Linc00210 drives Wnt/beta-catenin signaling activation and liver tumor progression through CTNNBIP1-dependent manner. Mol Cancer 2018; 17: 73.

15) Du P, Liu F, Liu Y, Shao M, Li X, Qin G. Linc00210 enhances the malignancy of thyroid cancer cells by modulating miR-195-5p/IGF1R/Akt axis. J Cell Physiol 2020; 235: 1001-1012.

16) Zhang S, Li P, Zhao L, Xu L. LINC00210 as a miR-328-5p sponge promotes nasopharyngeal carcinoma tumorigenesis by activating NOTCH3 pathway. Biosci Rep 2018; 38. pii: BSR20181168.

17) Hu Z, Chen J, Tian T, Zhou X, Gu H, Xu L, Zeng Y, Miao R, Jin G, Ma H, Chen Y, Shen H. Genetic variants of miRNA sequences and non-small cell lung cancer survival. J Clin Invest 2008; 118: 2600-2608.

18) Guan P, Yin Z, Li X, Wu W, Zhou B. Meta-analysis of human lung cancer microRNA expression profiling studies comparing cancer tissues with normal tissues. J Exp Clin Cancer Res 2012; 31: 54.

19) Ren Y, Huang W, Weng G, Cui P, Liang H, Li Y. LncRNA PVT1 promotes proliferation, invasion and epithelial-mesenchymal transition of renal cell carcinoma cells through downregulation of miR-16-5p. Onco Targets Ther 2019; 12: 2563-2575.

20) Liu Z, Wang Y, Wang L, Yao B, Sun L, Liu R, Chen T, Niu Y, Tu K, Liu Q. Long non-coding RNA AGAP2-AS1, functioning as a competitive endogenous RNA, upregulates ANXA11 expression by sponging miR-16-5p and promotes proliferation and metastasis in hepatocellular carcinoma. J Exp Clin Cancer Res 2019; 38: 194.

21) Cheng B, Ding F, Huang CY, Xiao H, Fei FY, Li J. Role of miR-16-5p in the proliferation and metastasis of hepatocellular carcinoma. Eur Rev Med Pharmacol Sci 2019; 23: 137-145.

22) Li Y, Wang H, Huang H. Long non-coding RNA MIR205HG function as a ceRNA to accelerate tumor growth and progression via sponging miR-122-5p in cervical cancer. Biochem Biophys Res Commun 2019; 514: 78-85.

23) Xu Y, Shen L, Li F, Yang J, Wan X, Ouyang M. MicroRNA-16-5p-containing exosomes derived from bone marrow-derived mesenchymal stem cells inhibit proliferation, migration, and invasion, while promoting apoptosis of colorectal cancer cells by downregulating ITGA2. J Cell Physiol 2019; 234: 21380-21394.

24) Zhang H, Yang K, Ren T, Huang Y, Tang X, Guo W. MiR-16-5p inhibits chordoma cell proliferation, invasion and metastasis by targeting Smad3. Cell Death Dis 2018; 9: 680.

25) Wang F, Mao A, Tang J, Zhang Q, Yan J, Wang Y, Di C, Gan L, Sun C, Zhang H. microRNA-16-5p enhances radiosensitivity through modulating Cyclin D1/E1-pRb-E2F1 pathway in prostate cancer cells. J Cell Physiol 2019; 234: 13182-13190.

26) Zhu C, Huang Q, Zhu H. Melatonin inhibits the proliferation of gastric cancer cells through regulating the miR-16-5p-Smad3 Pathway. DNA Cell Biol 2018; 37: 244-252.

27) Chen SS, Tang CH, Chie MJ, Tsai CH, Fong YC, Lu YC, Chen WC, Lai CT, Wei CY, Tai HC, Chou WY, Wang SW. Resistin facilitates VEGF-A-dependent angiogenesis by inhibiting miR-16-5p in human chondrosarcoma cells. Cell Death Dis 2019; 10: 31.

28) Krell A, Wolter M, Stojcheva N, Hertler C, Liesenberg F, Zapatka M, Weller M, Malzkorn B, Reifenberger G. MiR-16-5p is frequently down-regulated in astrocytic gliomas and modulates glioma cell proliferation, apoptosis and response to cytotoxic therapy. Neuropathol Appl Neurobiol 2019; 45: 441-458.

29) Ruan L, Qian X. MiR-16-5p inhibits breast cancer by reducing AKT3 to restrain NF-kB pathway. Biosci Rep 2019; 39. pii: BSR20191611.

30) Liu GP, Wang WW, Lu WY, Shang AQ. The mechanism of miR-16-5p protection on LPS-induced A549 cell injury by targeting CXCR3. Artif Cells Nanomed Biotechnol 2019; 47: 1200-1206.

31) Tutar L, Tutar E, Tutar Y. MicroRNAs and cancer; an overview. Curr Pharm Biotechnol 2014; 15: 430-437.

32) Zhou LK, Xu L, Ye J, Li D, Wang WS, Li XH, Wu LZ, Wang H, Guan FF, Li P. Cidea promotes hepatic steatosis by sensing dietary fatty acids. Hepatology 2012; 56: 95-107.

33) Fiebig HH, Berger DP, Winterhalter BR, Plowman J. In vitro and in vivo evaluation of US-NCI compounds in human tumor xenografts. Cancer Treat Rev 1990; 17: 109-117.

34) Behan FM, Iorio F, Picco G, Goncalves E, Beaver CM, Migliardi G, Santos R, Rao Y, Sassi F, Pinnelli M, Ansari R, Harper S, Jackson DA, McRae R, Pooley R, Wilkinson P, van der Meer D, Dow D, Buser-Doepner C, Bertotti A, Trusolino L, Stronach EA, Saez-Rodriguez J, Yusa K, Garnett MJ. Prioritization of cancer therapeutic targets using CRISPR-Cas9 screens. Nature 2019; 568: 511-516.

35) Wang X, Min S, Liu H, Wu N, Liu X, Wang T, Li W, Shen Y, Wang H, Qian Z, Xu H, Zhao C, Chen Y. Nf1 loss promotes Kras-driven lung adenocarcinoma and results in Psat1-mediated glutamate dependence. EMBO Mol Med 2019; 11. pii: e9856.

36) Fu QF, Liu Y, Fan Y, Hua SN, Qu HY, Dong SW, Li RL, Zhao MY, Zhen Y, Yu XL, Chen YY, Luo RC, Li R, Li LB, Deng XJ, Fang WY, Liu Z, Song X. Alpha-enolase promotes cell glycolysis, growth, migration, and invasion in non-small cell lung cancer through FAK-mediated PI3K/AKT pathway. J Hematol Oncol 2015; 8: 22.